LGR5 promotes invasion and migration by regulating YAP activity in hypopharyngeal squamous cell carcinoma cells

Zijia Zhu
First hospital of Jilin university
Shuyuan Yu
First hospital of Jilin university
Jihong Wen
Jilin university
Ping Wang (drwang_ping@126.com)
First hospital of Jilin university https://orcid.org/0000-0001-5191-3561

Primary research

Keywords: hypopharyngeal squamous cell carcinoma, LGR5, epithelial–mesenchymal transition, YAP phosphorylation

Posted Date: May 21st, 2020

DOI: https://doi.org/10.21203/rs.3.rs-28540/v1

Abstract

Background High leucine-rich repeat-containing G-protein coupled receptor 5 (LGR5) expression caused by an inflammatory microenvironment was reported to promote tumor proliferation and the epithelial–mesenchymal transition (EMT) in various malignant tumors, but those effects have not been studied in hypopharyngeal squamous cell carcinoma (HSCC) and the molecular mechanism remains unclear. Additionally, YAP/TAZ, an upstream or downstream factor of multiple signaling pathways, can promote tumor proliferation, invasion, and angiogenesis. Our study was aimed to determine whether YAP/TAZ is involved in the regulation of LGR5 expression in the inflammatory microenvironment.

Methods We stimulated FaDu cells, a hypopharyngeal squamous cell carcinoma cell line, with inflammatory medium. The expression levels of EMT-related proteins, LGR5, and p-YAP were detected by reverse transcription–polymerase chain reaction, western blotting, and immunofluorescence.

Results The results showed that LGR5 expression and the EMT process were significantly enhanced. The expression of EMT-related proteins was up-regulated, while that of p-YAP was decreased. After inhibiting the high LGR5 expression with short interfering RNA, the expression of EMT-related proteins was also down-regulated, while that of p-YAP was significantly increased. The use of verteporfin (VP), an inhibitor of YAP activity that promotes YAP phosphorylation, did not affect LGR5 expression.

Conclusions Our findings suggest that the inflammatory microenvironment leads to high LGR5 expression, up-regulating the expression of EMT-related proteins by inhibiting the YAP phosphorylation.

Background

The metastasis of hypopharyngeal squamous cell carcinoma (HSCC) is an important cause of its poor prognosis. In the past 20 years, the 5-year survival rate of patients with HSCC has never exceeded 55%. Because of the abundant blood supply and lymphatic drainage pathway around the head and neck, malignant tumors in this area are often prone to early metastasis.

In recent years, studies on malignant tumor infiltration, distant metastasis, and the epithelial–mesenchymal transition (EMT) have attracted much attention. Epithelial cells lose their original polarity, express the characteristics of mesenchymal cells, and acquire the ability of migration and anti-apoptosis. EMT is considered an important early event of tumor metastasis and is the main mode of metastasis and invasion of most malignant tumors[1]. Inhibition of the invasion and metastasis of tumor cells can be a new method for the treatment of squamous cell carcinoma. The underlying mechanism of EMT in head and neck tumors remains unclear and is of great research value.

The tumor development process is not only limited to local behavior but interactions with peripheral blood vessels, the extracellular matrix, surrounding normal cells, and related signaling molecules to form a complex regulatory network, namely the tumor microenvironment. Various signals in the tumor microenvironment play important roles in the survival, self-renewal, invasion, and metastasis of tumor

stem cells[2]. The major components of the tumor microenvironment include the hypoxia microenvironment and inflammatory microenvironment.

The inflammatory microenvironment and immunosuppressive microenvironment are two important components of the tumor microenvironment. The infiltration of immune cells and aggregation of inflammatory factors can induce the activation of oncogenes, promote the formation of tumor blood vessels, and promote the invasion, development and even metastasis of tumors[3, 4]. Leucine-rich repeat-containing G-protein coupled receptor 5 (LGR5), also known as GPR49, is a member of the G protein-coupled receptor protein family. LGR5 was initially found in the small intestine and hair follicles, is a marker of adult intestinal epithelial stem cells, and plays a crucial role in embryonic development[5]. In recent years, many studies have shown that LGR5 is highly expressed in multiple malignant tumor types, including colorectal cancer, ovarian cancer, hepatocellular carcinoma, basal cell carcinoma, and esophageal adenocarcinoma. Overexpression of LGR5 is significantly correlated with high clinical stage and metastatic status of breast cancer, indicating that LGR5 may be a promising prognostic marker for patients with breast cancer[6].LGR5 is expressed differently in different tissues but has not been studied in hypopharyngeal cancer.

The mechanism of action and regulation of different inflammatory factors secreted by inflammatory cells concerning the EMT phenotype of head and neck squamous epithelial cells under continuous inflammatory stimulation, as well as the correlation between the phenotypic transformation of LGR5 + stem cells and acquisition of EMT ability, warrant further study. In this study, the inflammatory cell supernatant produced by THP-1 macrophages under lipopolysaccharide (LPS) stimulation was applied to head and neck tumor cell lines, to establish the inflammatory microenvironment model of tumor cells, to isolate the LGR5 + cell subsets induced by inflammatory factors, and to determine the correlation between LGR5 and EMT by comparing and analyzing the phenotypic transformation ability of EMT with parental cells. By constructing a recombinant LGR5 plasmid to transfect tumor cells to overexpress LGR5 protein, the regulatory pathways and molecular mechanisms of EMT and phenotypic transformation of stem cells induced by inflammatory factors were verified.

YAP/TAZ is an important pair of transcription regulators that are highly active in most human malignancies. Recent studies have shown that YAP/TAZ plays a very important role in tumor development[7]. As an upstream or downstream factor of multiple signaling pathways, YAP/TAZ ultimately promotes tumor proliferation, invasion, and angiogenesis and metastasis. Normally, in mammals, the Hippo pathway kinase cascade leads to the phosphorylation of YAP/TAZ, trapping them in the cytoplasm, blocking their interaction with the TEA domain family member 1 (TEAD) family of transcription factors, and inhibiting cell proliferation and malignant transformation[8]. However, non-phosphorylated YAP/TAZ tends to be increased significantly in malignant tumor cells; they can enter the nucleus smoothly and regulate the expression of several genes related to proliferation, anti-apoptosis, and stem cell characteristics[9], including the secretory proteins connective tissue growth factor (CTGF) and CYR61[10, 11], AXL receptor tyrosine kinase[12], c-myc and survivin[12]. As a type of malignant tumor that seriously endangers human health, the role of YAP/TAZ in head and neck tumors has been rarely

studied. Because both LGR5 and YAP/TAZ are closely related to tumor development, the ability to invade and metastasize, as well as the properties of stem cells, we considered that a relationship may exist between the two. Therefore, verteporfin (VP), a benzoporphyrin derivative belonging to the porphyrin family, is a YAP inhibitor used in this study to disrupt the YAP-TEAD interaction[13].

It is important to clarify the complex relationship between LGR5/YAP signaling and the development of hypopharyngeal squamous cell carcinoma. Therefore, we investigated the expression change of LGR5 in FaDu cells under the inflammatory microenvironment. The invasion ability of FaDu cells was evaluated with LGR5 over-expression or knock-down treatment. This study tried to clarify the mechanism of LGR5/YAP signaling regulation in HSCC proliferation and invasion. The data could provide a special target for the clinical treatment of head and neck tumors.

Methods

Patients and specimens

Between February 2016 and March 2018, 47 patients with hypopharyngeal squamous carcinoma underwent tumor resection at the First Hospital of Jilin University and were included in this study. The clinical staging of these patients was classified according to the 8th edition of the Union for International Cancer Control stage classification. The diagnosis was made by chest radiography, nasopharyngeal and neck magnetic resonance imaging, nasopharyngeal fibroscopy, Epstein-Barr virus serological examination, and histopathological examination. The patient received no chemoradiotherapy before surgery. The tissue obtained from each patient contained both tumor tissues and corresponding adjacent nontumor tissues. We conducted all experiments according to the relevant guidelines and regulations. This study was approved by the institutional ethics committees of the First Hospital of Jilin University (Changchun, PR China). Written informed consent was obtained from each participant.

Cell culture

The human hypopharyngeal squamous cancer cell line FaDu and monocyte leukemia cell line THP-1 were obtained from Shanghai Zhongqiaoxinzhou Biotech Co., Ltd. (Shanghai, China). All the cells were grown in RPMI 1640 medium supplemented with 10% fetal bovine serum (FBS; Hyclone Laboratories, Inc., Logan, UT, USA), 1% penicillin, and 1% streptomycin and were maintained at 37°C in a humidified incubator with 5% CO_2.

Preparation of FaDu cells with LGR5 over-expression

FaDu cells were transfected with the LGR5 plasmid or control plasmid, which was purchased from GeneCopoeia (EX-Q0041-M03, EX-NEG-M03; Guangzhou, China). The LGR5 recombinant plasmid was constructed using pReceiver-M03 as the backbone plasmid and was inserted into the LGR5 cDNA coding sequence (NM_003667, ORF length: 2,724 bp). FaDu cells transfected with the LGR5 plasmid were

cultured in medium containing G418 for 14 d. The LGR5+ FaDu cells were collected to identify LGR5 over-expression using quantitative polymerase chain reaction (qPCR) and western blot assay.

Short interfering RNA (siRNA) transfection

FaDu cells were stimulated with inflammatory factors and then were transfected with siRNA oligo targeting the LGR5 gene, with a scrambled sequence as the control. Eight hours after transfection, the cell culture medium was replaced with RPMI 1640 containing 10% FBS and the cells were continued to incubate at 37°C for another 40 hours before the next step. An siRNA interference oligo sequence targeting the human LGR5 gene sequence (LGR5-homo-883) was designed and synthesized by Shanghai GenePharma Co., Ltd. The target sequence was UAAUAAGAG AAG GGUUGCCTT.

Cell proliferation assay

The proliferation ability of cells was measured by the CCK-8 assay using Cell Counting Kit (Yeasen, Shanghai). Different groups of cells were inoculated into 96-well plates at the density of 1,000 cells per well. After 24 hours, the CCK-8 reagent was added, followed by incubation at 37°C for 1 hour. The absorbance at 450 nm was recorded using a microplate reader.

Immunofluorescence staining

Cells to be observed were inoculated on glass slides and rinsed three times with phosphate-buffered saline (PBS) 24 hours later, and then the cells were fixed in 4% paraformaldehyde at room temperature for 30 minutes. The cells were washed three times with PBS and then were incubated with 0.1% Triton X-100, blocked in 5% goat serum for 1 hour, and then were incubated overnight with 1:100 diluted primary antibody at 4°C. Next, the cells were washed with PBS and then were incubated with 1:400 diluted secondary antibody in the dark for 1 hour at room temperature, followed by washing three times with PBS. The slides were sealed with glycerine at a concentration of 50% and then were observed and photographed with a laser confocal microscope (Fluo-View FV1000; Olympus, Japan).

Wound healing assay

FaDu cells of different groups were inoculated in 24-well plates and scratched with a 200-μl pipette tip when the plate was completely covered. PBS solution was used to wash away floating cell debris. Next, photos of the freshly scratched surfaces were taken. Thereafter, the cells were cultured at 37°C and 5% CO_2 for 24 hours and then were photographed again to compare the healing of each “wound”. The scratch spacing at each time point was measured by Image J software [$R_M = (W_2\text{-}W_1)/W_2 \times 100\%$ (RM=relative mobility, W_1=initial cell covering rate, W_2=final cell covering rate)]. The relative mobility of the cells at each time point was calculated with 0-hour scratch spacing as a reference, and the experimental results were analyzed using SPSS17.0 statistical software. The counting data were expressed as a percentage, while the measurement data were expressed as ±S. One-way analysis of variance was used for comparison of multi-group mean values.

Cell migration assay

Cell invasion ability was determined by the Transwell assay. Cell suspensions with concentrations of 5×10^5/ml were prepared with 0.1% FBS in RPMI 1640 medium. Next, 5×10^4 cells were placed in the upper chamber (pore size: 8 μm; Millipore, Billerica, MA, USA) precoated with 1:4 diluted Matrigel (Yeasen, Shanghai, China). The lower chamber was filled with RPMI 1640 medium containing 20% FBS as an inducer. After incubation for 24 hours, the cells in the upper chamber and Matrigel were erased with cotton swabs, and the lower cells were stained with 0.5% crystal violet. Cell invasion was observed under an optical microscope (magnification, ×40).

Real-time quantitative PCR (qPCR) detection system

Total RNA was extracted from each group using Trizol reagent, and the RNA integrity was verified by agarose gel electrophoresis. The RNA was reversed transcribed into cDNA using the Transcriptor First Strand cDNA Synthesis Kit (Cat.04897030001). Additionally, cDNA was amplified using FastStart Essential DNA Green Master, Cat.06924204001, (Roche, Indianapolis, IN, USA). The specific primer designs are shown in Table 1. The real-time PCR protocol was performed according to our previous studies[14]. The target gene mRNA level was normalized to that in β-actin, and the relative mRNA levels were calculated using the formula: Fold change = $2^{-\triangle\triangle CT}$.

Western blot analysis

The proteins were extracted with cell lysate buffer (T-PER Tissue Protein Extraction Reagent containing phosphatase inhibitor (Halt Protease and Single-Use Inhibitor Cocktail; 78442; Thermo). The proteins were separated using 10% SDS-polyacrylamide gel electrophoresis and then were transferred to PVDF membranes. The membrane was blocked with 5% non-fat milk powder for 1 hour and then was incubated with antibodies overnight at 4°C, washed three times with TBST, and then incubated with horseradish peroxidase-labeled secondary antibody at room temperature for 1.5 hours. The primary antibodies were as follows: LGR5 Polyclonal antibody (Cat# A10545), TWIST1 Polyclonal antibody (Cat# A7314), YAP Polyclonal antibody (Cat# A1001), pYAP Polyclonal antibody (Cat# AP0489), and SNAIL Polyclonal antibody (Cat# A5243), all from *ABclonal* Biotechnology Co., Ltd, China. β-Actin monoclonal antibody (Cat# ab8226; Cambridge, MA, USA) was used as a working internal control. ECL reagent (Thermo Fisher Scientific, Waltham, MA, USA) was used to visualize protein bands, and images were obtained using a Dolphin-C hemi Mini image system (Wealtec Corp., Sparks, NV, USA). Gray values for each protein band were analyzed using Image J analysis software, and relative protein levels were calculated using β-actin as an internal control.

Immunohistochemistry

The tissue sections were dewaxed and hydrated, rinsed with 0.01 mol/L of PBS, and heated in 0.01 mol/L of citrate buffer (pH=6.0) for 10 minutes for antigen repair. After washing with PBS, 3% hydrogen peroxide was added and then the sections were incubated for 15–20 minutes to remove endogenous

peroxidase activity. The sections were blocked with goat serum for 15–20 minutes and then were incubated with LGR5 monoclonal antibody (1:300) at 4°C overnight. The biotinylated secondary antibody IgG was added dropwise onto the sections, followed by incubation at temperature for 15–20 minutes, incubation with streptomycin-labeled horseradish enzyme for another 15–20 minutes, application of DAB (diaminobiphenyl; Bioss, Beijing, China) for color development, and re-staining with hematoxylin for 1 minute. The LGR5 staining intensity (PI) = cell staining intensity (SI) × percentage of positive cells (PP) and was scored as follows: 0~5 points, negative; 6~12 points, positive. The SI results were scored as follows: 0, no staining; 1, yellow staining; 2, brown staining; 3, brown staining. The PP result judgment was scored as follows: 0%, 0 points; < 15%, 1 point; 16%~50%, 2 points; 51%~75%, 3 points; > 75%, 4 points.

Statistical analysis

All the data were collected from at least three independent experiments. Results were analyzed using SPSS17.0 statistical software and are expressed as means ± standard deviation (SD). Student's t-test, one-way analysis of variance, and multivariate analysis of variance were used to analyze data as appropriate. A value of $P < 0.05$ was considered statistically significant. Chi-squared test was used to evaluate the correlation between LGR5 and clinicopathological features.

Results

Expression of LGR5 in HSCC tissues

In 47 tissue pairs, LGR5 was highly expressed in 68.1% (32/47) of HSCC tumor tissues and 34.0% (16/47) of the adjacent normal tissues. The positive rate of LGR5 protein in HSCC tumor tissues was significantly higher than that in adjacent non-cancerous tissues (68.1% vs. 34.0%, respectively; $P<0.001$; Table 2 and Figure 1).

The inflammatory microenvironment affects the proliferation and migration ability of FaDu cells.

We obtained culture medium rich in cytokines by adding LPS (8 μg/ml) to the culture medium of THP-1 cells (Figure 2A). We chose to harvest the supernatant at 24 hours after stimulation because the amount of tumor necrosis factor (TNF)-α, the most abundant cytokine, reached its peak at this time. We tried to dilute the supernatant in various proportions, but the CCK-8 assay showed that the diluted supernatant had little effect on tumor cell viability. The medium was then used to simulate an inflammatory microenvironment. The cell viability of FaDu cells treated with the inflammatory microenvironment was compared with that of the untreated control group by the CCK-8 assay. The optical density (OD) of each group was measured 24 hours after administration at a 450-nm wavelength. The OD value was significantly increased in the treatment group. The proliferation of FaDu cells in the experimental group was 24.36% higher than that in the control group. Hence, the results showed that the inflammatory microenvironment can promote the proliferation of FaDu cells (Figure 2B). We also conducted wound healing experiments, which showed that the proliferation and migration of tumor cells in the

inflammatory microenvironment were significantly stronger than those of the control group. At 24 hours, the relative mobility of cells in the blank control group was 50.00±4.243%, while that in the experimental group was 72.25±5.439%. A significant difference was found between the groups (P<0.01) (Figure 2C,D). Finally, the Transwell invasion assay was performed. This experiment indicated that the ability of HSCC to invade under the stimulation of the inflammatory microenvironment was significantly enhanced compared with that in the control group. The number of transmembrane cells in the experimental group was (55.00±7.071)/HP while that in the control group was (24.20±7.294)/HP (Figure 2E,F).

The inflammatory microenvironment leads to high LGR5 expression in FaDu cells.

The experimental results of immunofluorescence showed that, compared with the control group, LGR5 expression in the treatment group was significantly higher. Additionally, the morphology of tumor cells in the inflammatory microenvironment showed clear transformation. The cell morphology changed from oval to spindle shaped, giving them a stronger ability to invade (Figure 3A). qPCR was used to detect LGR5 expression. The experimental results showed great changes after stimulation of the inflammatory microenvironment. The LGR5 expression level increased significantly compared with that of the original value (Figure 3B). Using actin as the internal control, the LGR5 mRNA expression level in the experimental group was increased by 2.27 times for 12 hours and 2.88 times for 24 hours compared with the initial value (P<0.01; Figure 3B). Additionally, we conducted western blotting experiments to detect LGR5 mRNA expression. The results showed that its expression level was upregulated in the inflammatory microenvironment (Figure 3C,D). Compared with the control group, the expression level of LGR5 protein in the experimental group was increased by 2.41 times for 12 hours and by 2.32 times for 24 hours (P<0.01).

The expression levels of EMT-related genes in FaDu cells with the over-expression or gene-knockdown of LGR5.

To investigate the biological significance of LGR5 in HSCC, the cells were transfected with LGR5 overexpression plasmids. The relative expression levels of EMT-related proteins were measured by western blotting. The levels of vimentin, twist, and snail in the LGR5 overexpression group were markedly upregulated compared with those in the control group. The expression levels of vimentin, twist, and snail were increased by 2.65, 1.65, and 2.53 times, respectively (Figure 4A,B). The expression levels of vimentin, twist, and snail in FaDu cells transfected with LGR5 siRNA or siRNA NC were also detected by western blotting. The levels of vimentin, twist, and snail were decreased by 1.96, 2.56, and 3.41 times, respectively, in the LGR5 siRNA group compared with those in the siRNA NC group (Figure 4C,D).

Over-expression or gene-knockdown of LGR5 influenced the ability of migration and invasion of FaDu cells in vitro

The invasion and migration of HSCC cells were significantly enhanced after they were transfected with the LGR5 overexpression plasmid. The relative mobility of the cells and number of transmembrane cells in the blank control group were 33.40±4.506% and (34.40±5.177)/HP, respectively, while the values in the experimental group transfected with the LGR5 overexpression plasmid were 59.60±6.542% and (68.20±13.41)/HP, respectively. In the group of cells transfected with empty plasmids, the two values were 29.00±7.176% and (30.80±10.40)/HP, respectively ($P<0.01$) (Figure 5A–D). As shown in Figure 7F and H, the relative mobility of cells in the empty plasmid-transfected group was 52.80±8.167% while that of cells stimulated only by the inflammatory microenvironment was 56.60±8.620%. Additionally, little difference was found between the groups. Nevertheless, when the expression of LGR5 was inhibited, the inflammatory microenvironment cannot enhance cell migration and invasion. As shown in Figure 5E–H, the relative mobility of cells and number of transmembrane cells were 35.00±5.612% and (28.80±4.147)/HP, respectively. However, the number of transmembrane cells that were stimulated by the inflammatory microenvironment without LGR5 inhibition was (64.80±7.225)/HP ($P<0.001$).

LGR5 inhibits the phosphorylation of YAP.

The expression of LGR5 and p-YAP was detected by immunofluorescence and western blotting. The phosphorylation level of YAP was decreased by 2.31 times when LGR5 was overexpressed compared with that in the control group ($P<0.001$) (Figure 6B,C). However, after the addition of siRNA to inhibit the high expression of LGR5 caused by the inflammatory microenvironment, the phosphorylation level of YAP was 2.49 times higher than that of cells treated with the inflammatory microenvironment alone ($P<0.001$) (Figure 6B,D). The use of VP to increase the phosphorylation level of YAP did not affect LGR5 expression (Figure 6A–D).

Regarding immunofluorescence analysis, after inflammatory microenvironment stimulation, siRNA transfection, and VP treatment, many cells died, and obvious nuclear fragmentation was observed (Figure 6A-f,B-f). Two possible causes of cell death exist: 1. siRNA has a strong inhibitory effect on LGR5 expression, resulting in low LGR5 expression, which reduces the tolerance of cells to VP and ultimately cell death; 2. An unknown reaction occurred between VP and the transfection reagent, resulting in the formation of toxic substances, leading to cell death.

VP impairs the ability of FaDu cells to invade and migrate.

We conducted wound healing experiments, and the results showed that the migration of LGR5-overexpressed FaDu cells after VP stimulation was weaker than that of the control group. At 24 hours, the relative mobility of cells in the control group was 131.0±14.53% while that in the VP experimental group was 40.33±4.163% ($P<0.01$; Figure 7A,B). Next, the Transwell invasion assay was performed. The invasive ability of LGR5-overexpressed FaDu cells after VP stimulation was predominantly diminished compared with that in the control group. The number of transmembrane cells in the experimental group with VP was (47.67±5.508)/HP while that in the control group was (70.67±3.786)/HP (Figure 7 C,D).

Discussion

High LGR5 expression has been previously reported to be closely related to tumor proliferation and invasion and has been detected in various malignancies. Studies on liver cancer, colorectal tumors, basal cell carcinoma, ovarian cancer, and other tumors[15] have shown that LGR5 promotes cell proliferation and invasion in tumor cells, and leads to tumor stem cell-like characteristics, resulting in a poor prognosis. Other studies have shown that LGR5 plays an inhibitory role in CRC progression in colorectal cancer[16]. LGR5 expression in different tumors is different while that in hypopharyngeal cancer has not been studied. According to our study, LGR5 expression in HSCC is higher than that in normal tissues surrounding the tumor (Figure 1).

A large number of inflammatory factors, such as interleukin (IL)-1, IL-6, and TNF-α, exists in the inflammatory microenvironment. Studies have shown that these cytokines are important factors that promote the generation, proliferation, and invasion of various tumor cells[17, 18]. In the IL-1 study, wild-type and IL-1β-knockout (KO) mice were inoculated with B16 melanoma cells. The IL-1β-knockout mice did not develop tumors, but the wild-type mice developed melanoma, which caused deaths[18]. Thus, the inflammatory microenvironment plays a key role in the occurrence and development of malignant tumors. In this study, LPS was used to stimulate THP-1 cells to produce inflammatory factors to simulate the inflammatory microenvironment. The proliferation and invasion of FaDu cells were enhanced in the inflammatory microenvironment. After the inflammatory microenvironment was used to stimulate FaDu cells, LGR5 expression was detected by western blotting. After 12 hours of stimulation, LGR5 expression was significantly up-regulated and did not continue to increase over time (Figure 3C,D). However, when siRNA was used to inhibit the high LGR5 expression in FaDu cells caused by inflammatory microenvironmental stimulation, the cell viability was significantly reduced, and the ability of proliferation and invasion was weakened. Therefore, the inflammatory microenvironment likely causes high LGR5 expression in HSCC, thus promoting the proliferation and invasion of tumor cells.

We confirmed through scratch and Transwell experiment that high LGR5 expression can promote the migration and invasion of tumor cells. Subsequently, we detected the expression of various EMT-related proteins, among which the expression levels of vimentin, twist, and snail were regulated by LGR5. However, E-cadherin and N-cadherin[19], which play key roles in the EMT of many tumors, were found not to be regulated by LGR5 after multiple tests in the HSCC we studied. No significant changes were observed in the expression of E-cadherin and N-cadherin regardless of LGR5 overexpression or inhibition (data not shown). Therefore, we believe that, in HSCC, LGR5 regulates the cell EMT process through vimentin, twist, and snail, rather than by involving E-cadherin and N-cadherin, as in most cases.

Previous studies have shown that the YAP-TEAD interaction is an important factor that promotes the proliferation, migration, and invasion of tumor cells[20, 21]. Many studies have demonstrated that the hyperfunction of YAP and TAZ may promote the proliferation of tumor cells[22] and the process of EMT, which includes high expression of YAP/TAZ or nuclear enrichment, has been detected in melanoma, breast cancer, and other tumors[23]. YAP can be transported to the nucleus and bind with transcription

factors such as TEADs to promote the expression of target genes[20]. The YAP/TAZ pathway is associated with the expression of many genes. For example, studies have shown that VASN (vasorin) in thyroid cancer promotes the EMT of thyroid cancer cells by triggering the YAP/TAZ pathway[24]. TRPV4 (transient receptor potential cation channel subfamily V member 4) was found to be very important for the nuclear transport of YAP/TAZ. By regulating YAP/TAZ nuclear translocation, TRPV4 promotes EMT in normal mouse primary epidermal keratinocytes, resulting in changes in the expression levels of EMT-related markers, such as E cadherin, N cadherin, and α-smooth muscle actin [25, 26]. Therefore, YAP is regulated by some genes and the expression of some genes. We considered whether a relationship exists between LGR5 and YAP-TEAD. Additionally, studies have shown that specific siRNA silencing of YAP in the human colon cancer cell line HCT116 can affect the recruitment of p300 protein, reduce the acetylation of p53AIP1 target genomic protein, and lead to the delay or reduction of p73-mediated apoptosis[27]. Thus, YAP has different effects in different tumors. The tumor we studied was hypopharyngeal squamous carcinoma. Using various experiments, we proved that the inflammatory microenvironment-induced high LGR5 expression in FaDu cells and LGR5 overexpression lead to the hyperfunction of YAP/TAZ and enhanced proliferation, migration, and invasion of tumor cells.

YAP can be phosphorylated by VP, and phosphorylated YAP binds to proteins and remains in the cytoplasm[28, 29]. Therefore, the destruction of YAP/TAZ nuclear transport by VP can inhibit the EMT process to a certain extent[30], a finding that was also confirmed in this study. In our study, high LGR5 expression could lead to the reduction of p-YAP, and the expression level of EMT-related protein was up-regulated (Figure 4B). The use of VP to increase the phosphorylation level of YAP had little effect on LGR5 expression, but the invasion ability of tumor cells was significantly decreased (Figure 6A). Therefore, we believe that the inflammatory microenvironment causes high LGR5 expression, which will inhibit the phosphorylation of YAP, resulting in markedly increased YAP-TEAD binding, high expression of EMT-related proteins, and enhanced invasion and metastasis ability of tumor cells. Low expression of the YAP gene by shRNA[31, 32] and interference of the formation of the YAP-TEAD complex by VP[33, 34] have been reported to induce apoptosis. In this study, VP was also used to phosphorylate YAP, but many cells died after siRNA inhibition of LGR5 expression; however, few of the cells died in the LGR5 over-expression group (Figure 6A-f,B-f). Therefore, we hypothesized that LGR5 expression may lead to apoptosis resistance caused by the functional inhibition of YAP.

Conclusions

In conclusion, we have demonstrated for the first time that the inflammatory microenvironment can lead to high LGR5 expression in HSCC, and high LGR5 expression can promote the proliferation and invasion of tumor cells by inhibiting the phosphorylation of YAP. Therefore, LGR5, YAP, and the relationship between LGR5 and YAP phosphorylation can be used as targets for the treatment of HSCC and have potential clinical value in prognosis.

Abbreviations

HSCC, hypopharyngeal squamous cell carcinoma

EMT, epithelial mesenchymal transformation

VP, verteporfin

LGR5, leucine-rich repeat-containing G-protein coupled receptor 5

LPS, lipopolysaccharide

YAP/TAZ, Yes-associated protein

TEAD, TEA domain family member 1

CTGF, connective tissue growth factor

CYR61, cysteine-Rich Angiogenic Inducer 61

FaDu, hypopharyngeal squamous cell carcinoma cell line

Declarations

Availability of data and materials

The datasets used and/or analyzed during the current study are available from the corresponding author upon reasonable request.

Acknowledgements

Not applicable.

Funding

This study was supported by grants from Jilin Provincial Science& Technology Development (Grant No. 20150101171JC).

Contributions

ZZ wrote the manuscript and performed the experiments, SY participated in study esign and data collection, JW and PW participated in study design and data collection.All authors read and approved the final manuscript.

Ethics approval and consent to participate

This study was approved by the institutional ethics committees of the First Hospital of Jilin University (Changchun, PR China). Written informed consent was obtained from each participant.

Consent for publication

Not applicable.

Competing interests

The authors declare that they have no competing interests.

References

1. Mittal V. Epithelial Mesenchymal Transition in Tumor Metastasis. Annu Rev Pathol. 2018;13:395–412.
2. Okada F. Inflammation-related carcinogenesis: current findings in epidemiological trends, causes and mechanisms. Yonago Acta Med. 2014;57(2):65–72.
3. Sullivan NJ, Sasser AK, Axel AE, Vesuna F, Raman V, Ramirez N, Oberyszyn TM, Hall BM. Interleukin-6 induces an epithelial-mesenchymal transition phenotype in human breast cancer cells. Oncogene. 2009;28(33):2940–7.
4. Zhu Y, Cheng Y, Guo Y, Chen J, Chen F, Luo R, Li A. Protein kinase D2 contributes to TNF-α-induced epithelial mesenchymal transition and invasion via the PI3K/GSK-3β/β-catenin pathway in hepatocellular carcinoma. Oncotarget. 2016;7(5):5327–41.
5. Cao HZ, Liu XF, Yang WT, Chen Q, Zheng PS. LGR5 promotes cancer stem cell traits and chemoresistance in cervical cancer. Cell Death Dis. 2017;8(9):e3039.
6. Hou MF, Chen PM, Chu PY. LGR5 overexpression confers poor relapse-free survival in breast cancer patients. BMC Cancer. 2018;18(1):219.
7. Zanconato F, Cordenonsi M, Piccolo S. YAP/TAZ at the Roots of Cancer. Cancer Cell. 2016;29(6):783–803.
8. Zhao B, Li L, Tumaneng K, Wang CY, Guan KL. A coordinated phosphorylation by Lats and CK1 regulates YAP stability through SCF(beta-TRCP). Genes Dev. 2010;24(1):72–85.
9. Wu L, Yang X. Targeting the Hippo Pathway for Breast Cancer Therapy. Cancers (Basel). 2018;10(11):422.
10. Zhao B, Ye X, Yu J, Li L, Li W, Li S, Yu J, Lin JD, Wang CY, Chinnaiyan AM, Lai ZC, Guan KL. TEAD mediates YAP-dependent gene induction and growth control. Genes Dev. 2008;22(14):1962–71.
11. Lai D, Ho KC, Hao Y, Yang X. Taxol resistance in breast cancer cells is mediated by the hippo pathway component TAZ and its downstream transcriptional targets Cyr61 and CTGF. Cancer Res. 2011;71(7):2728–38.
12. Xu MZ, Chan SW, Liu AM, Wong KF, Fan ST, Chen J, Poon RT, Zender L, Lowe SW, Hong W, Luk JM. AXL receptor kinase is a mediator of YAP-dependent oncogenic functions in hepatocellular carcinoma. Oncogene. 2011;30(10):1229–40.

13. Brodowska K, Al-Moujahed A, Marmalidou A, Meyer Zu Horste M, Cichy J, Miller JW, Gragoudas E, Vavvas DG. The clinically used photosensitizer Verteporfin (VP) inhibits YAP-TEAD and human retinoblastoma cell growth in vitro without light activation. Exp Eye Res. 2014;124:67–73.
14. Li Y, Wang P, Zhao J, Li H, Liu D, Zhu W. HMGB1 attenuates TGF-β-induced epithelial-mesenchymal transition of FaDu hypopharyngeal carcinoma cells through regulation of RAGE expression. Mol Cell Biochem. 2017;431(1–2):1–10.
15. Xu L, Lin W, Wen L, Li G. Lgr5 in cancer biology: functional identification of Lgr5 in cancer progression and potential opportunities for novel therapy. Stem Cell Res Ther. 2019;10(1):219.
16. Jang BG, Kim HS, Chang WY, Bae JM, Kim WH, Kang GH. Expression Profile of LGR5 and Its Prognostic Significance in Colorectal Cancer Progression. Am J Pathol. 2018;188(10):2236–50.
17. Sfanos KS, Yegnasubramanian S, Nelson WG, De Marzo AM. The inflammatory microenvironment and microbiome in prostate cancer development. Nat Rev Urol. 2018;15(1):11–24.
18. Voronov E, Shouval DS, Krelin Y, Cagnano E, Benharroch D, Iwakura Y, Dinarello CA, Apte RN. IL-1 is required for tumor invasiveness and angiogenesis. Proc Natl Acad Sci U S A. 2003;100(5):2645–50.
19. Kourtidis A, Necela B, Lin WH, Lu R, Feathers RW, Asmann YW, Thompson EA, Anastasiadis PZ. Cadherin complexes recruit mRNAs and RISC to regulate epithelial cell signaling. J Cell Biol. 2017;216(10):3073–85.
20. Marti P, Stein C, Blumer T, Abraham Y, Dill MT, Pikiolek M, Orsini V, Jurisic G, Megel P, Makowska Z, Agarinis C, Tornillo L, Bouwmeester T, Ruffner H, Bauer A, Parker CN, Schmelzle T, Terracciano LM, Heim MH, Tchorz JS. YAP promotes proliferation, chemoresistance, and angiogenesis in human cholangiocarcinoma through TEAD transcription factors. Hepatology. 2015;62(5):1497–510.
21. Noguchi S, Saito A, Nagase T. YAP/TAZ Signaling as a Molecular Link between Fibrosis and Cancer. Int J Mol Sci. 2018;19(11):3674.
22. Xu W, Yang Z, Xie C, Zhu Y, Shu X, Zhang Z, Li N, Chai N, Zhang S, Wu K, Nie Y, Lu N. PTEN lipid phosphatase inactivation links the hippo and PI3K/Akt pathways to induce gastric tumorigenesis. J Exp Clin Cancer Res. 2018;37(1):198.
23. Park JH, Shin JE, Park HW. The Role of Hippo Pathway in Cancer Stem Cell Biology. Mol Cells. 2018;41(2):83–92.
24. Bhandari A, Guan Y, Xia E, Huang Q, Chen Y. VASN promotes YAP/TAZ and EMT pathway in thyroid carcinogenesis in vitro. Am J Transl Res. 2019;11(6):3589–99.
25. Sharma S, Goswami R, Zhang DX, Rahaman SO. TRPV4 regulates matrix stiffness and TGFβ1-induced epithelial-mesenchymal transition. J Cell Mol Med. 2019;23(2):761–74.
26. Sharma S, Goswami R, Rahaman SO. The TRPV4-TAZ mechanotransduction signaling axis in matrix stiffness- and TGFβ1-induced epithelial-mesenchymal transition. Cell Mol Bioeng. 2019;12(2):139–52.
27. Strano S, Monti O, Pediconi N, Baccarini A, Fontemaggi G, Lapi E, Mantovani F, Damalas A, Citro G, Sacchi A, Del Sal G, Levrero M, Blandino G. The transcriptional coactivator Yes-associated protein drives p73 gene-target specificity in response to DNA Damage. Mol Cell. 2005;18(4):447–59.

28. Lee Y, Kim NH, Cho ES, Yang JH, Cha YH, Kang HE, Yun JS, Cho SB, Lee SH, Paclikova P, Radaszkiewicz TW, Bryja V, Kang CG, Yuk YS, Cha SY, Kim SY, Kim HS, Yook JI. Dishevelled has a YAP nuclear export function in a tumor suppressor context-dependent manner. Nat Commun. 2018;9(1):2301.
29. Dasari VR, Mazack V, Feng W, Nash J, Carey DJ, Gogoi R. Verteporfin exhibits YAP-independent anti-proliferative and cytotoxic effects in endometrial cancer cells. Oncotarget. 2017;8(17):28628–40.
30. Li N, Feng Y, Hu Y, He C, Xie C, Ouyang Y, Artim SC, Huang D, Zhu Y, Luo Z, Ge Z, Lu N. Helicobacter pylori CagA promotes epithelial mesenchymal transition in gastric carcinogenesis via triggering oncogenic YAP pathway. J Exp Clin Cancer Res. 2018;37(1):280.
31. Lin C, Xu X. YAP1-TEAD1-Glut1 axis dictates the oncogenic phenotypes of breast cancer cells by modulating glycolysis. Biomed Pharmacother. 2017;95:789–94.
32. Wang X, Wu B, Zhong Z. Downregulation of YAP inhibits proliferation, invasion and increases cisplatin sensitivity in human hepatocellular carcinoma cells. Oncol Lett. 2018;16(1):585–93.
33. Wei H, Wang F, Wang Y, Li T, Xiu P, Zhong J, Sun X, Li J. Verteporfin suppresses cell survival, angiogenesis and vasculogenic mimicry of pancreatic ductal adenocarcinoma via disrupting the YAP-TEAD complex. Cancer Sci. 2017;108(3):478–87.
34. Pan W, Wang Q, Zhang Y, Zhang N, Qin J, Li W, Wang J, Wu F, Cao L, Xu G. Verteporfin can Reverse the Paclitaxel Resistance Induced by YAP Over-Expression in HCT-8/T Cells without Photoactivation through Inhibiting YAP Expression. Cell Physiol Biochem. 2016;39(2):481–90.

Tables

Table 1. qPCR Primers

Gene name	Forward Primer	Reverse Primer
LGR5	5’-CCTGCTTGACTTTGAGGAAGACC-3’	5’-CCAGCCATCAAGCAGGTGTTCA-3’
Snail1	5'-TTTCTGGTTCTGTGTCCTCTG-3'	5'-TGTCAGCCTTTGTCCTGTAGC-3'
Twist1	5'-AGTCCGCAGTCATACGAGGAG-3'	5'-GACCTAGTAGAGGAAGTCGATG-3'
Vimentin	5’-AGTCCACTGAGTACCGGAGAC-3’	5’-CATTTCACGCATCTGGCGTTC-3’
Yap	5’–GCTACAGTGTCCCTCGAACC–3’	5’-CCGGTGCATGTGTCTCCTTA-3’
β-actin	5'-TGGCACCCAGCACAATGAA-3'	5'- CTAAGTCATAGTCCGCCTAG-3'

Table 2. Expression of LGR5 in HSCC tumor tissue and adjacent normal tissue

Variables		LGR5	P
	Positive	Negative	
Cancerous tissue(X)	32	15	0.001
Adjacent normal tissue (Y)	16	31	

Figures

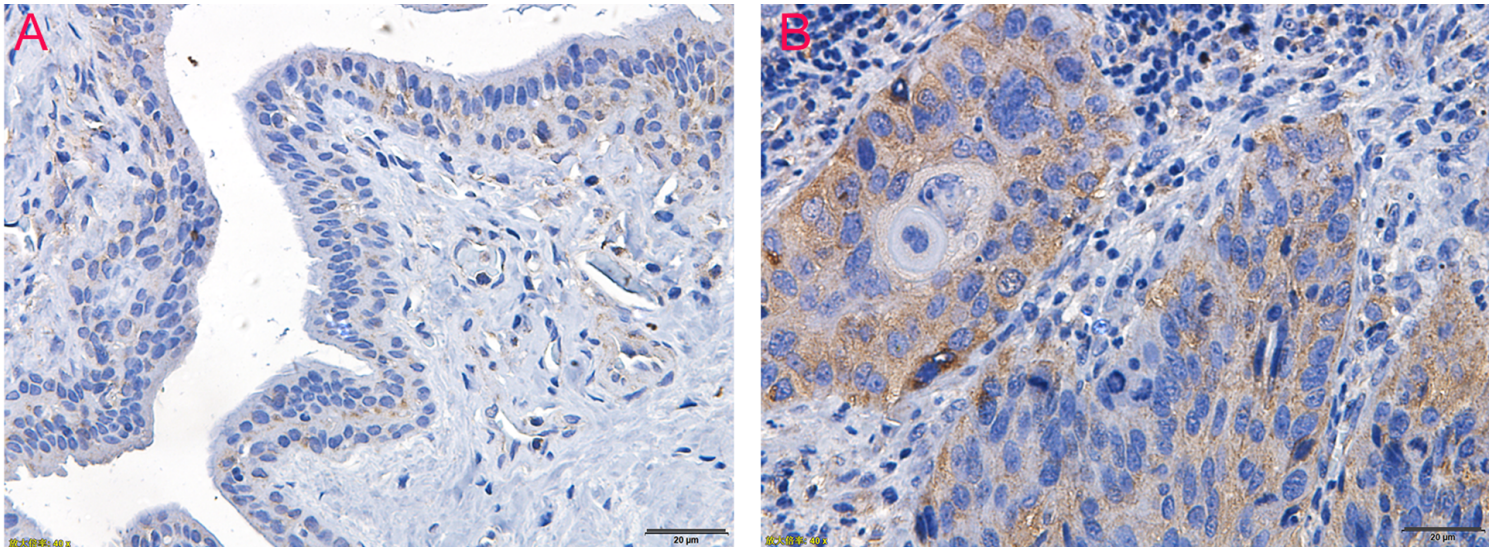

Figure 1

Immunohistochemical staining of LGR5 in HSCC and normal oropharyngeal mucosa tissues. LGR5 expression was lower in normal mucosal tissues than in tumor tissues. LGR5 is mainly expressed in the cytoplasm of tumor cells. A, B: Scale bar=20 μm.

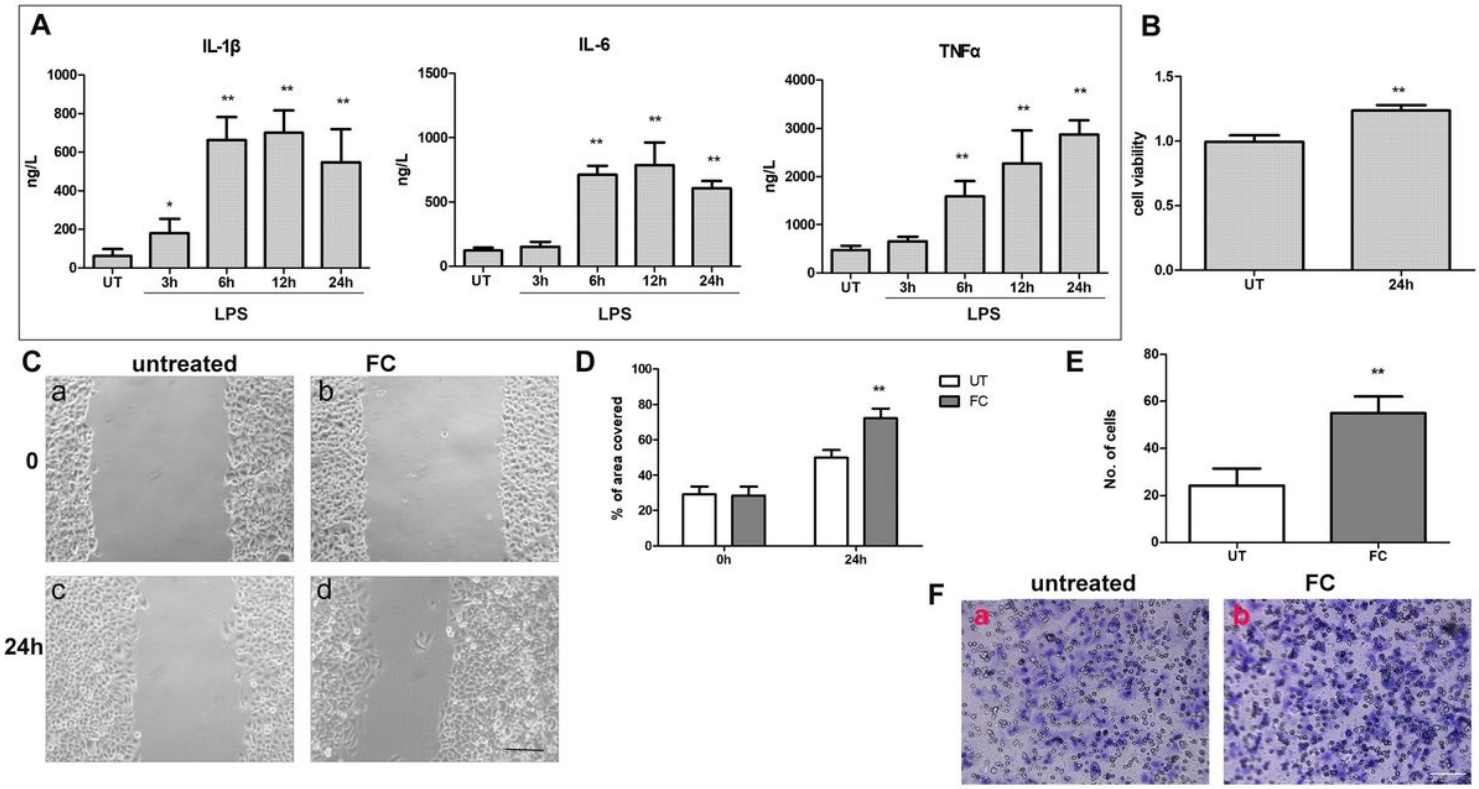

Figure 2

Effect of the inflammatory microenvironment on tumor cell invasion and proliferation. A: Change in the IL-1β, IL-6, and TNF-α levels in THP-1 cells under LPS stimulation. B: Cell viability under the inflammatory microenvironment after 24 hours using the CCK8 assay. C-D: Cell migration was observed under the inflammatory microenvironment after 24 hours using the wound healing assay. Scale bar=50 μm. E-F: Cell invasion was observed using the Transwell chamber set. Scale bar=20 μm. Statistical significance is denoted by *P<0.05, **P<0.01, FC group vs UT group. UT: untreated group; FC: inflammatory microenvironment.

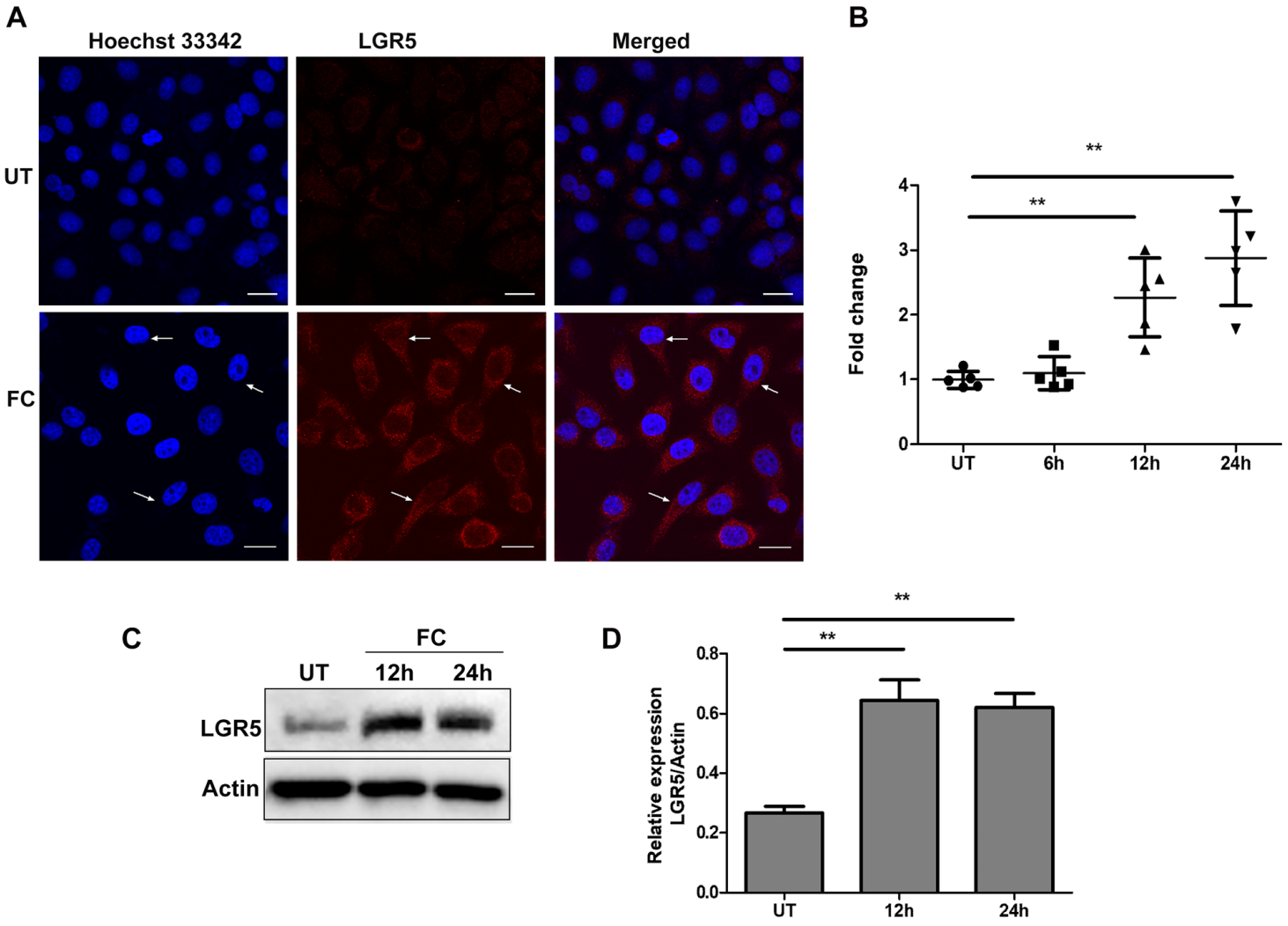

Figure 3

The inflammatory microenvironment affects LGR5 expression in FaDu cells. A: Representative imaging of LGR5 expression in FaDu cells by immunofluorescence assay. FaDu cells stained for Hoechst 33342 (blue) and LGR5 (red) after treatment with the inflammatory microenvironment or control group are shown. The arrows indicate FaDu cells with stromal-like phenotypic changes. Scale bar=20 μm. B: The expression level of LGR5 in FaDu cells was analyzed by reverse transcription-quantitative PCR after 6, 12, and 24 hours of treatment with the inflammatory microenvironment. C-D: The experimental group was treated with the inflammatory microenvironment for 12 and 24 hours. Western blotting was used to analyze LGR5 expression in FaDu cells. Quantification (D) and representative blots (C) are shown. Statistical significance is denoted by **P<0.01. UT: untreated group; FC: inflammatory microenvironment.

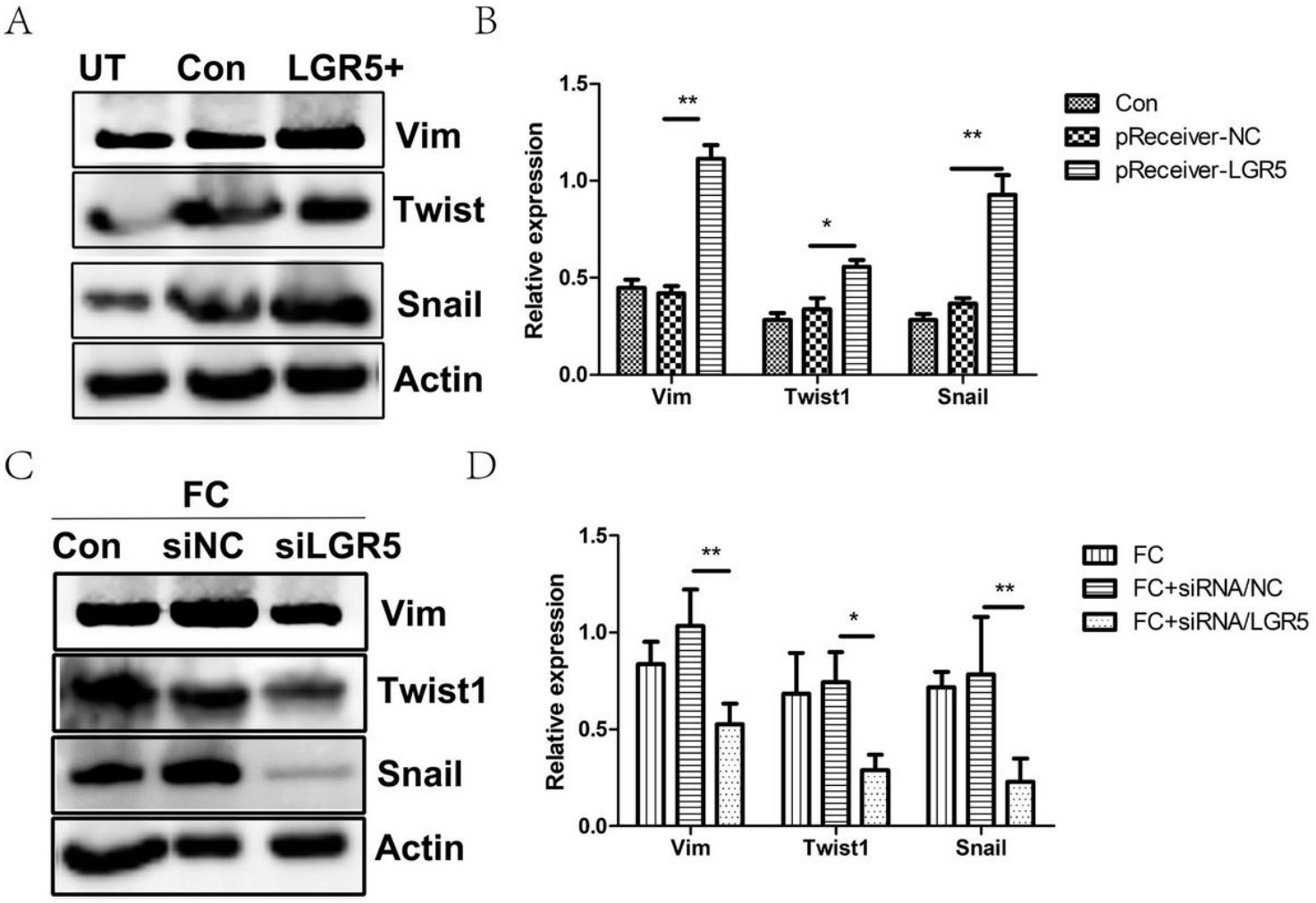

Figure 4

Expression levels of EMT-related genes. A-B: The expression levels of the EMT-related genes vimentin, twist, and snail were detected in FaDu/FGR5+ cells by western blotting. Quantification (B) and representative blots (A) are shown. C-D: FaDu cells with FC stimulation were transfected with LGR5 siRNA or siRNA NC. The expression levels of vimentin, twist, and snail were analyzed by western blotting. Quantification (D) and representative blots (C) are shown. Statistical significance is denoted by *P<0.05, **P<0.01. UT: untreated group; FC: inflammatory microenvironment; siNC: negative control siRNA; siLGR5: LGR5 siRNA.

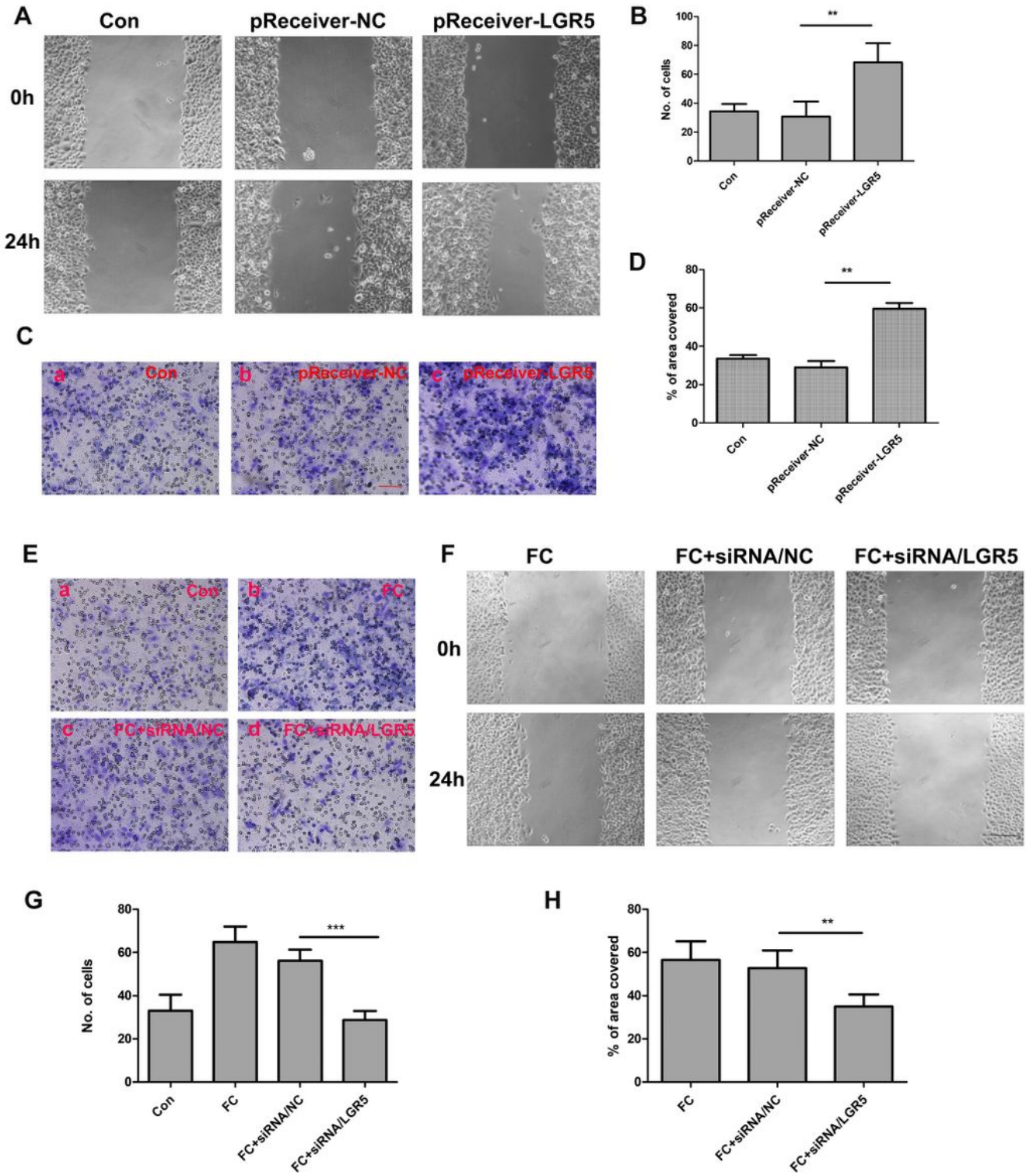

Figure 5

Effects of LGR5 overexpression on tumor cell invasion and proliferation. A, D, F, H: The effect of LGR5 expression on cell migration was detected by the wound healing assay. The results showed that the cell migration ability was enhanced after LGR5 overexpression. Quantification (D) and representative imaging (A) are shown. Scale bar=50 μm. B, C, E, G: The Transwell assay was used to test the invasiveness of the cells. According to the quantitative (B) and representative imaging(C) results, both LGR5 overexpression

and the inflammatory microenvironment can lead to enhanced cell invasion ability. However, when LGR5 expression is inhibited, the invasion ability stimulated by FC was reduced. Scale bar=20 μm. Statistical significance is denoted by **P<0.01,***P<0.001. Con: control group; pReceiver-NC: negative control plasmid; pReceiver-LGR5: LGR5 overexpression plasmid; FC: inflammatory microenvironment; siRNA/NC: negative control siRNA; siRNA/LGR5: LGR5 siRNA

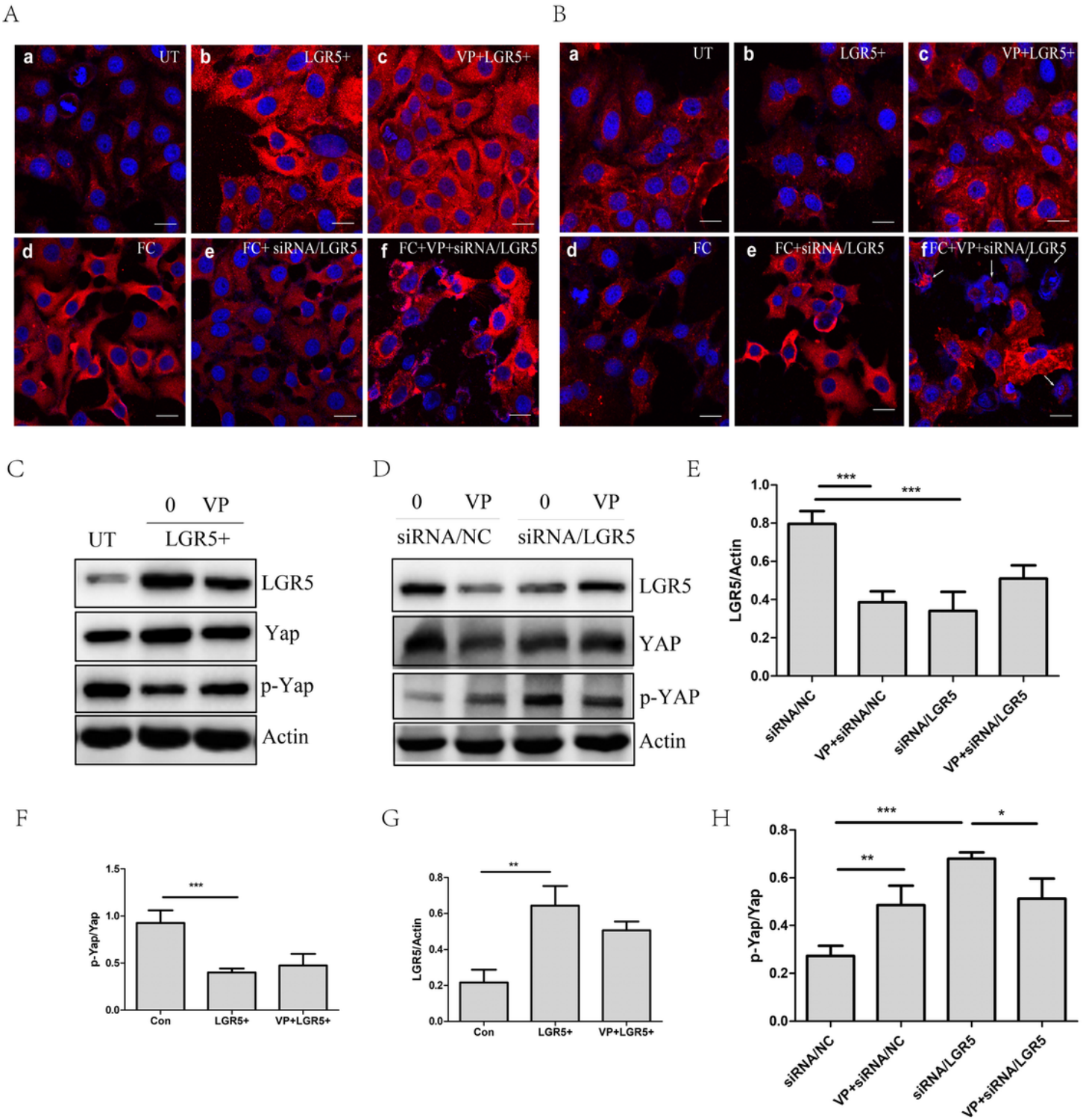

Figure 6

Relationship between the phosphorylation of YAP and LGR5 expression. A: LGR5 expression was detected by immunofluorescence assay. FaDu cells were subjected to immunofluorescent staining for Hoechst 33342 (blue) and LGR5 (red). The cells were subjected to various treatments: transfection with LGR5 plasmids or stimulation with the inflammatory microenvironment; inhibition of LGR5 expression by siRNA; inhibition of YAP phosphorylation by VP. The experimental results of immunofluorescence are shown in Figure 6A. Scale bar=20 μm. 6B: The expression of p-YAP was detected by immunofluorescence assay. FaDu cells were subjected to immunofluorescent staining for Hoechst 33342 (blue) and phosphorylated YAP (red). C: Western blotting was used to detect LGR5 or p-YAP expression in LGR5-overexpressed cells or siRNA/LGR5-transfected FaDu cells. Statistical significance is denoted by**P<0.01,***P<0.001. UT: untreated group; FC: inflammatory microenvironment; VP: verteporfin; LGR5+: stable cell lines overexpressing LGR5; siRNA/NC: negative control siRNA; siRNA/LGR5: LGR5 siRNA.

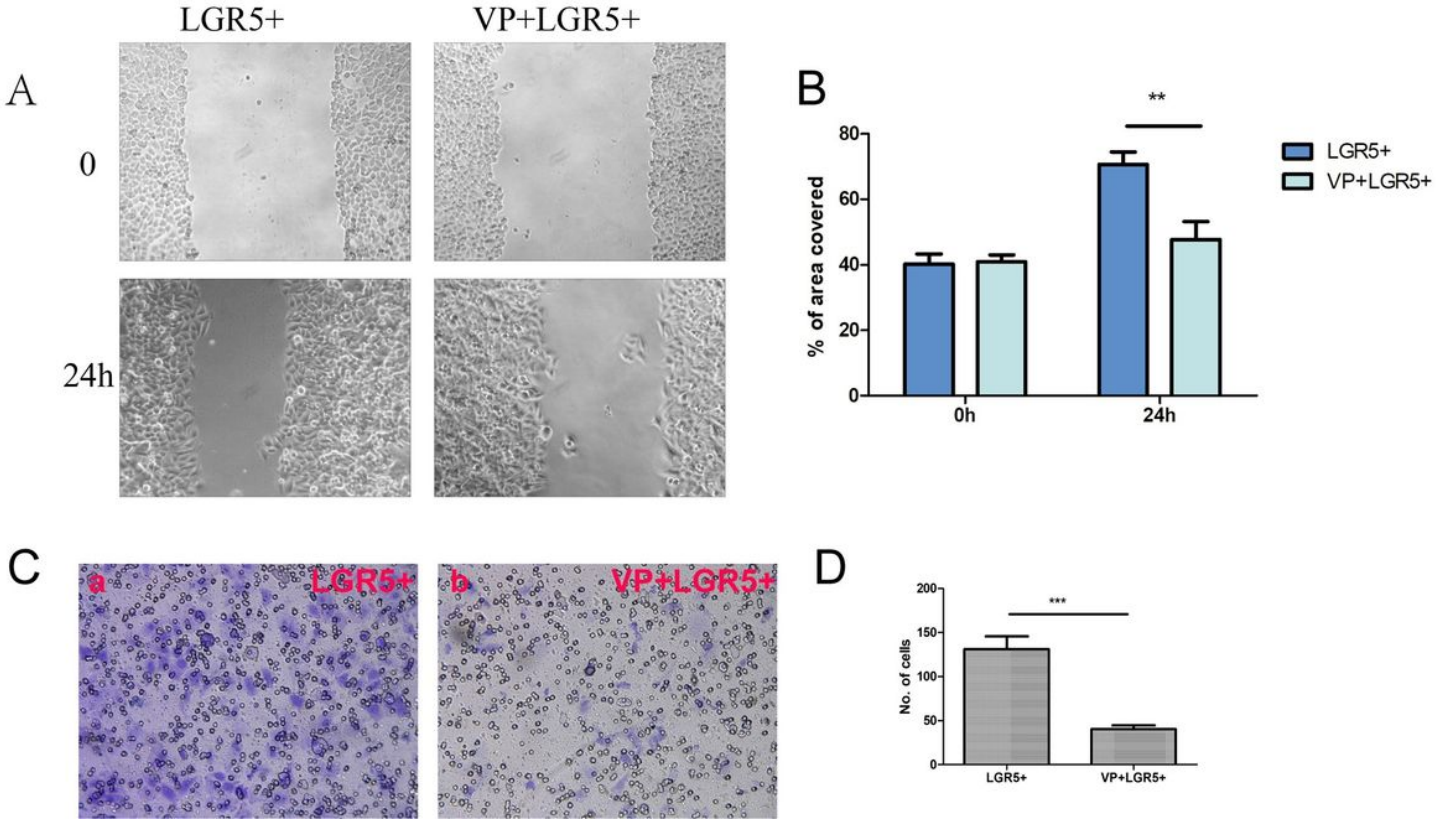

Figure 7

VP affects the invasion and migration of FaDu cells. A-B. The ability of cell migration was measured by the wound healing test. Quantification (B) and representative imaging (A) are shown. Scale bar=50 μm. C-D. The invasiveness of FaDu cells was detected by the transwell assay. The pore diameter of the chamber is 8 μm. Quantification (D) and representative imaging (C) are shown. Scale bar=20 μm. The mean between the groups was compared by independent samples t-test. Statistical significance is denoted by **P<0.01,***P<0.001.